Calibration of the spectral radiant power responsivity of windowed pyroelectric radiometers from 785 nm to 14 μm

Jinan Zeng and Leonard Hanssen
National Institute of Standards and Technology
100 Bureau Drive, Gaithersburg, MD, USA 20899-8441
Email: jzeng@nist.gov; Tel: 301-975-4473, Fax: 301-975-6991

ABSTRACT

As part of the optical detector characterization program at the Optical Technology Division at NIST, we have established a capability for the calibration of spectral radiant power responsivity in the infrared from 785 nm to 14 μm. We have used our facilities to characterize two commercial pyroelectric radiometers with KRS5 windows. The calibration methodology consists of the determination of the responsivity at single wavelength tie points together with relative spectral responsivity measurements. Responsivity tie points at 785, 1064, 1320, 1600, 2000 and 10600 nm are obtained against the NIST ACR-L1 absolute cryogenic radiometer as well as a domed pyroelectric transfer standard, using an OPO tunable laser and a stabilized CO_2 laser as sources. The spatial variation of the responsivity of the test radiometers has also been measured. This enables us to minimize the uncertainties due to interference fringes from the KRS5 window. The relative spectral responsivity curves for the two radiometers are obtained indirectly through measurement of the detector absorptance with an FTIR-based integrating sphere reflectometer. In order to obtain the actual absorptance at the detector from the reflectance measurements, an individual KRS5 window and a bare detector were also measured. The results are compared and the uncertainty budgets will be discussed.

Keywords: Pyroelectric radiometer with KRS5 window, spectral radiant power responsivity, absolute cryogenic radiometer, domed pyroelectric transfer standard, OPO tunable laser, stabilized CO_2 laser, FTIR, detector absorptance

1. INTRODUCTION

A capability for the calibration of spectral radiant power responsivity in the infrared from 785 nm to 14 μm has been established at the Optical Technology Division at NIST to meet the increasing demand for detector calibration at different wavelengths of interest. The IR detector characterization capabilities include electrical tests of noise equivalent power (NEP) and frequency dependence and optical characterization such as spatial uniformity of responsivity, angular dependence of responsivity, and linearity, etc. We have used our facilities to characterize two commercial pyroelectric radiometers with KRS5 windows. The calibration methodology consists of the determination of the responsivity at single wavelength tie points together with relative spectral responsivity measurements. The technical challenges of the calibration for the KRS5 windowed pyroelectric radiometers results from the spatial uniformity and interference fringes at different wavelengths and with various beam geometries, and the accurate measurement of the detector absorptance through the window due to the unknown reflectance of the window in use. The relative spectral responsivity curves for the two radiometers are obtained indirectly through measurement of the detector absorptance with an FTIR-based integrating sphere reflectometer. In order to obtain the actual absorptance at the detector from the reflectance measurements, an individual KRS5 window and a bare detector were also measured. To obtain multiple responsivity tie points from 785 to 10600 nm, an absolute cryogenic radiometer (ACR) and a domed pyroelectric transfer standard[1, 2] are applied with a tunable optical parametric oscillator (OPO) laser system (700 to 2200 nm) and independent multiple lasers, including diode lasers (785 and 1320 nm) and a stabilized CO_2 laser. The ACR and pyroelectric transfer standard based calibration systems are adopted to provide several wavelengths for comparison and confirmation of the relative spectral results from the reflectometer measurements.

Infrared Spaceborne Remote Sensing and Instrumentation XVI, edited by Marija Strojnik,
Proc. of SPIE Vol. 7082, 70820Y, (2008) · 0277-786X/08/$18 · doi: 10.1117/12.799665

2. FACILITIES AND EXPERIMENAL DESCRIPTION

2.1 OPO tunable laser and ACR calibration system[3]

Fig 1. shows a schematic configuration for ACR-based spectral responsivity measurement using tunable lasers. The main advantages of laser-based calibrations are very accurately known wavelengths, a very small bandwidth (i.e., a high spectral purity), a high signal-to-noise ratio (particularly for absolute radiometers), stabilization by electro-optic (EO) or acousto-optic modulation, very low stray light level, and good beam geometry (low beam divergence and easy alignment). The tunable IR sources used for the tie-point responsivity measurements mainly consists of a periodically poled $LiNbO_3$ (PPLN) OPO pumped by a mode-locked Nd:YVO_4 laser with a pulse duration of 7.5 ps and a repetition rate of 220MHz, and an LBO OPO pumped by the second harmonic of the Nd:YVO_4 laser. The PPLN OPO tunable laser can cover 1350 to 5000 nm, and the LBO OPO laser tunes from 700 nm to 2000 nm in the output power level from several hundred mW to 1 W. As part of the suite of sources, a cw CO, CO_2 and isotope CO_2 lasers adds the long wavelength ranges of 5000 to 7000 nm, 9000 to 12000 nm, and 8000 to 11000 nm, respectively.

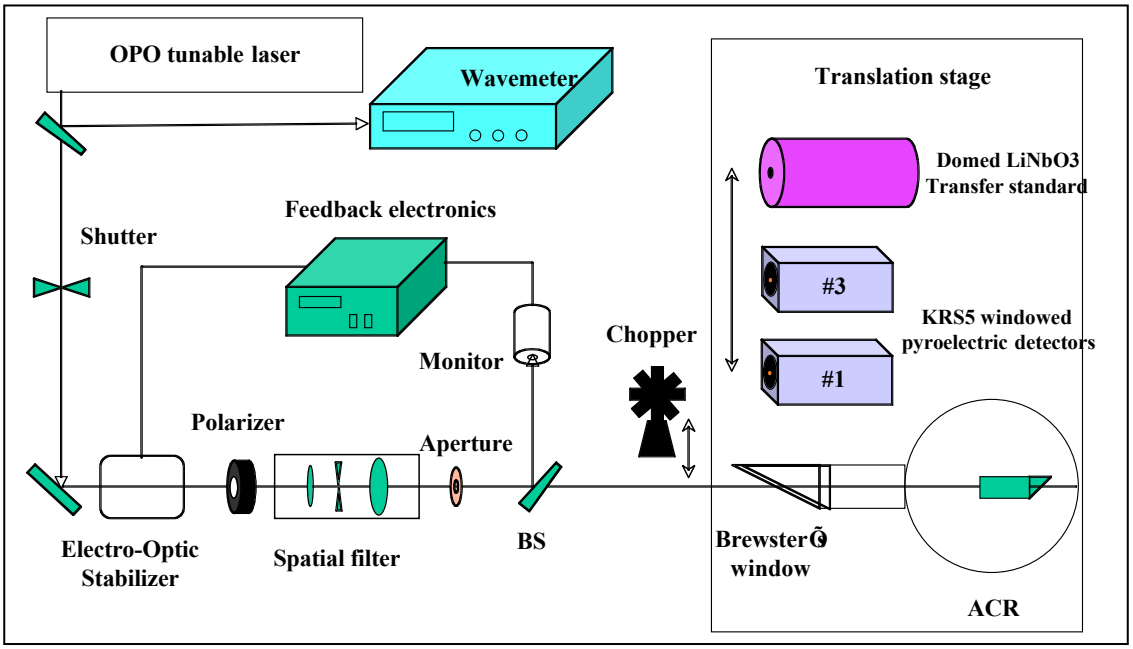

Fig. 1 Schematic configuration for ACR-based spectral responsivity measurements using tunable lasers.

As illustrated in Fig. 1, the laser radiation from a tunable laser is input to a beamsplitter (Si or Ge) to redirect part of the beam into a wavemeter to accurately measure the wavelength of the laser. There is a controllable shutter placed in the path to allow a measurement of the background. Then the laser beam passes through an electro-optic stabilizer and an attenuating polarizer to reduce the instability of the beam intensity to less than 0.5%. The adjustable polarizer is also used to minimize the reflection from the Brewster window on the ACR. A spatial filter is used to optimize the beam profile. The output generates a large diffraction Airy pattern. An aperture is applied to trim the beam and select only the central spot to form a collimated beam of 700 to 800 μm diameter for input to the ACR and detector under test (DUT). Part of the input beam is also sent into a monitor detector (Si, InGaAs, or extended InGaAs) by a wedged beam splitter. The signal from this monitor detector is utilized as a feedback for the EO stabilizer. And it also can be used to correct the residual laser drift. Both the ACR and radiometers under test are mounted on a 600 mm travel translation stage. For each radiometer under test, there is a set of XY translation stages for relative positioning. A beam profiler and a pyroelectric camera are used to maintain the alignment of laser beam tuned to different wavelengths. A chopper is applied for the calibration of pyroelectric radiometers (AC mode), while the ACR operates in DC mode.

2.2 IR detector characterization and calibration facilities

In order to obtain the uncertainties associated with the radiometer's responsivity during both its calibration and the calibration transfer to other radiometers, we have established characterization capacities of radiometers. The frequency- and temperature-dependent responsivity, signal-gain stability, and noise characteristics are measured in a separate Ambient Infrared Detector Characterization Facility (not described here). The Infrared Detector Evaluation Facility (IDEF)[4] is used for measurement of the spatial non-uniformity of responsivity, linearity, angular responsivity, absolute responsivity, stability, and repeatability. The Fourier Transform Infrared Spectrophotometry Facility (FTIS) [5,6] is used to derive the spectral absorptance (proportional to the relative spectral responsivity) of the detectors from spectral reflectance measurements.

2.2.1 Infrared Detector Evaluation Facility (IDEF) using multi-lasers

As shown in Fig. 2, the experimental apparatus for IDEF consists of four parts: (1) multiple laser sources including a stabilized CO_2 laser and 785 nm and 1.32 μm diode lasers, (2) a beam manipulation and control unit for beam profile optimization and polarization control, (3) a motorized detector translation-rotation system, and (4) a signal acquisition and processing unit. A stabilized CO_2 laser can achieve stability of its output power to within ± 0.5 % in the short term (minutes) and 1-2 % in the long term (hours) with a stabilization system based on an electro-mechanical translator. An optical detector implemented in the laserhead sends a feedback signal to a dither stabilization circuit to realize this function. The CO_2 laser, with a maximum output power of 4 W, can be grating tuned from 9.17 μm to 10.86 μm. The stabilized laser output beam is passed through a spatial filter to improve the beam profile and collimation. Several ultrathin film neutral density filters (OD 2, 3, and 4) mounted in a filter wheel are PC-controlled to coarsely attenuate the beam power and a two-polarizer attenuator is used to fine-tune the output power intensity. The achievable power levels span the range from nW to W. A motorized halfwave plate is used to manipulate the polarization of the laser beam. A mirror chopper plays a role as a beam splitter for feedback of part of laser beam into a monitor pyroelectric detector used to ratio out the residual drift.

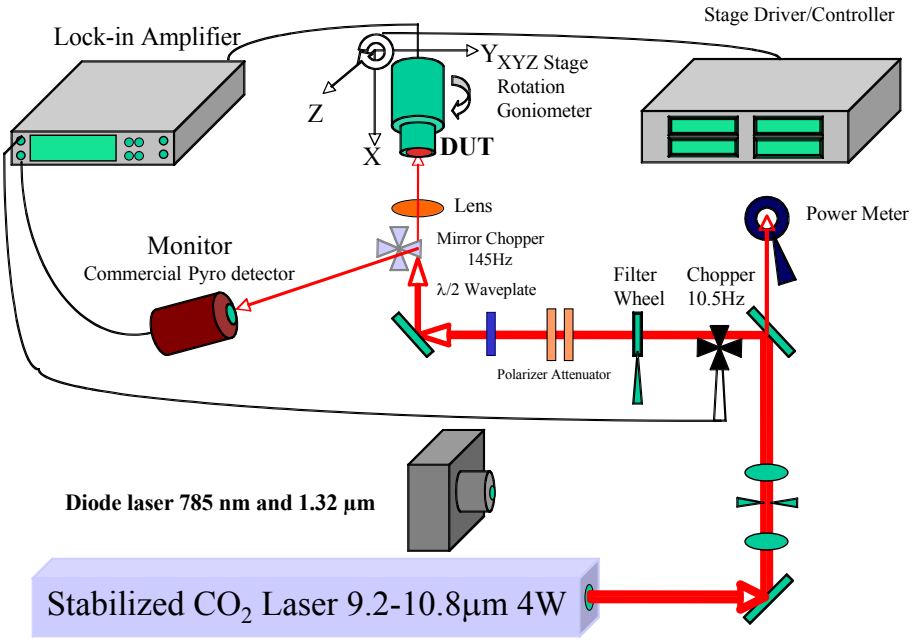

Fig. 2 Schematic diagram of the IDEF system

The IDEF system can be used to perform characterization measurements such as spatial uniformity of responsivity, angular dependence of responsivity, linearity, and frequency dependence of responsivity, as well as the calibration tie-points of absolute responsivity at different wavelengths of 785 nm, 1.32 μm, and 10.6 μm.

2.2.2 Fourier Transform Infrared Spectrophotometry Facility (FTIS)

In the FTIS facility, a Fourier transform infrared (FTIR) spectrometer and integrating sphere are used to measure reflectance spectra from 800 nm to 20 µm. Detailed descriptions of the instrumentation are described elsewhere.[5, 6] The reflectance of the windowed detectors was measured, as well as the reflectance of a third bare detector and the reflectance and transmittance of a third KRS5 window. Measurements were performed in two configurations of the FT spectrometer for overlapping mid-infrared and near-infrared spectral regions. Due to the small size of the detectors (5 mm diameter), several system characterization measurements were required and performed for each spectral range. From the complete sets of measurements, the effective spectral absorptance of the detectors is obtained, where "effective" absorptance is defined as the ratio of the flux absorbed by the detector element to the flux input to the detector package (i.e. onto the KRS5 window).

3. CALIBRATION RESULTS AND DISCUSSION

3.1 IDEF characterization and calibration

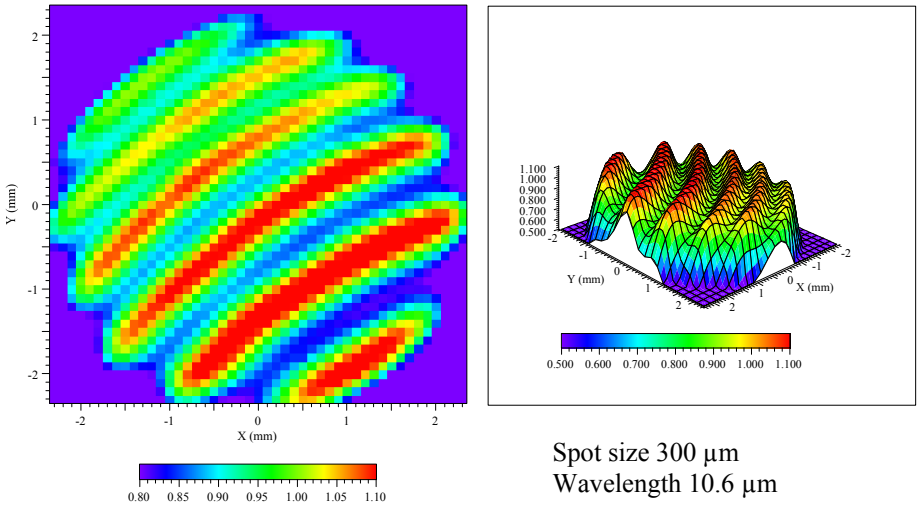

Fig. 3 Spatial non-uniformity of responsivity of the KRS5 windowed pyroelectric radiometer #1 at 10.6 µm

Fundamental characterization measurements of detectors are necessary prior to the responsivity measurement for tie-points. The spatial uniformity measurements of the relative responsivity for the two radiometers denoted herein as "Pyro #1 and Pyro #3" (out of an original set of 4), were measured by using a beam spot of 300 µm with intervals of 100 µm at 10.6 µm. A map of the spatial variation of Pyro #1 over an area of 5 mm in diameter is shown in Fig. 3. The interference fringes are dependent on the thickness variation of the detector window, beam geometry, wavelength and temperature. The KRS5 window, with a reflectance of approximately 15% per surface, is slightly wedged, which leads to the interference fringes. At 10.6 µm, several fringes are observed across the surface, the amplitude of the fringes masks the underlying variation of the detector element itself. The interference structure is an indication of the variation of the window thickness across its surface. The regular and apparent interference fringe patterns have been obtained with a period of about 1.4 mm along the diagonal direction in Fig. 3. The Pyro#1 and #3 detectors exhibit different orientations of fringe patterns. Pyro #1 has a fringe pattern as shown in Fig. 3 while Pyro #3 has a pattern oriented in the Y direction. It means the KRS5 windows were mounted without regard to the wedge orientation. Cross-sectional scans of both detectors are shown in Fig. 4 (a) and (b). We increased the spot size to reduce the amplitude of the fringes, by moving the detector away from the input beam focus. This, however, prevents us from seeing the local response variation of the detector element itself. Also, as the spot size increases, some of the light misses the detector, and the inter-reflection between the detector surface and the window and the can holding the window can change. We averaged the results over several complete fringe orders to obtain responsivity values. At shorter wavelengths the apparent fringe amplitude is

decreased, because the fringe spacing is smaller, approaching the laser spot size. If the detectors are used in a high resolution system such as one with laser sources, similar interference effects can be expected.

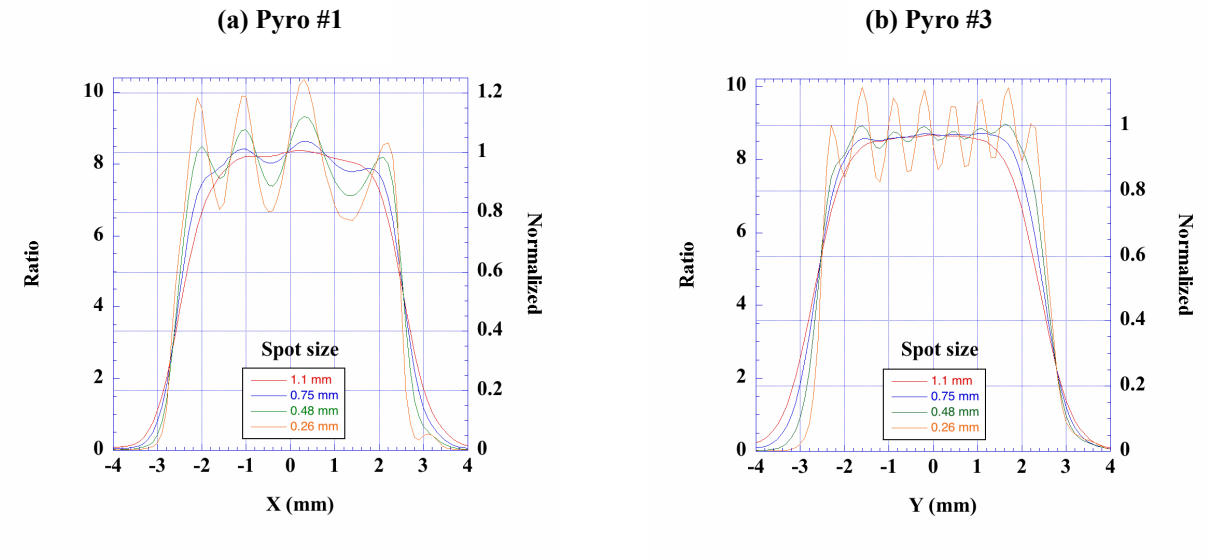

Fig. 4 Variation of interference fringes with beam spot size at 10.6 μm

3.2 ACR calibration

The final results of the IR SIRCUS absolute responsivity calibrations are plotted in Fig. 5 (a) for Pyro #1 and (b) for Pyro #3. The error bars indicate the expanded (*k=2*) uncertainties from the table for each data point. The legend indicates the particular traceability path: ACR means direct calibration of the test detector against the ACR, LiNbO3 means direct calibration against the transfer standard LiNbO3 detector (which was previously calibrated via a traceability chain to a second ACR,[1] and LiNbO3/ACR means indirect comparison to the transfer standard detector.

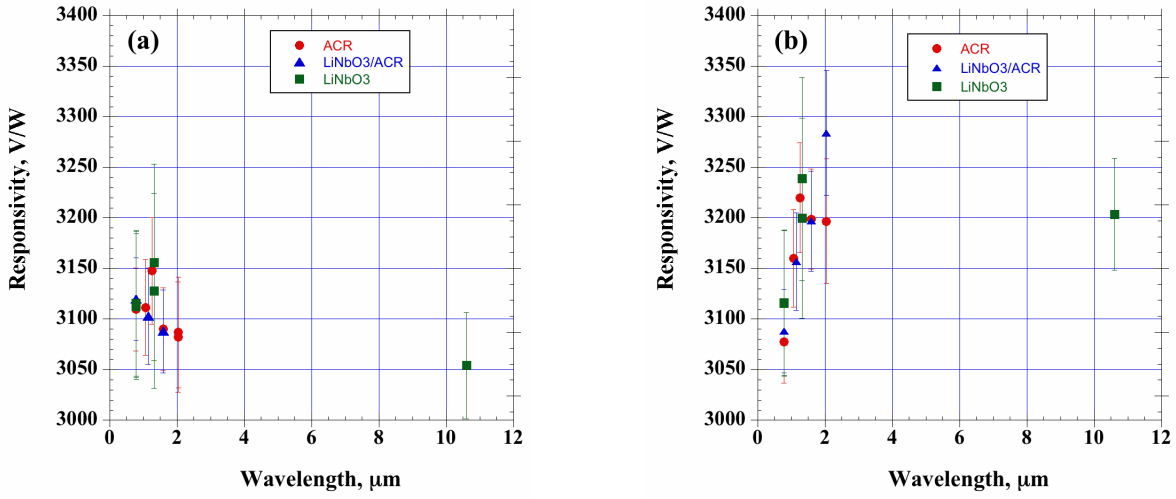

Fig. 5 Absolute responsivity of pyroelectric test detectors (a) Pyro #1 and (b) Pyro #3.

In principle, the absolute spectral responsivity only needs to be measured at a single wavelength, since we assume that the pyroelectric detector's response is directly proportional to the absorptance of the detector's surface. But when combined with a window, the effective absorptance of the detector becomes the quantity that is directly proportional to

the responsivity. Furthermore, we cannot measure the effective absorptance of the detector directly. By calibrating the absolute spectral responsivity at several wavelengths across the spectrum, we are able to assess and validate the calculated effective absorptance spectra as well as the assumption that they are directly proportional to the responsivity. All the data shown in Fig. 5 are used in the final spectral responsivity calibration results.

3.3 FTIR reflectometry

To obtain the spectral dependence of the pyroelectric detector responsivity, we measured the reflectance of the detector units Pyro #1 and #3, and we separately measured the components of a third detector: the reflectance of the bare detector surface and the reflectance and transmittance of the KRS5 window. The instrument we use for measurement of the detector reflectance is a custom infrared integrating sphere that uses an FITR spectrophotometer source.[2] Using this instrument with our measurement methodology, we can obtain the absolute spectral reflectance of samples. We match our input beam spot size to underfill the pyroelectric detectors, which have a 5 mm diameter detecting surface area.

3.3.1 Measurement sequence description

For alignment purposes, the system is typically operated with a visible beam, enabling us to view the spot on the sample directly. However, the KRS5 window makes this method difficult. Hence the detectors were mounted on motorized translation stages and scanned both vertically and horizontally to center the spot on the sample. The motorized stages block the rear access to the reference port on the integrating sphere. This, in turn, prevented us from performing our standard reference measurement. Hence we performed the reflectance measurements in a relative mode, comparing to a gold mirror reference, which was calibrated in a separate measurement.

For small samples, especially for those with low reflectance levels, we need to correct for the light that overfills the detector area of interest, but is reflected from either outside the sample port, or inside the port but outside the detector area. This overfill light is captured by the sphere and measured. We deal with this by making all measurements with an aperture placed in front of the detector. We make measurements of 1) each detector, 2) a second gold standard mirror, and 3) an "empty" aperture with nothing behind it. The aperture is fixed on the sphere sample port and does not move between these measurements. The reflectance values obtained for the two detectors are obtained from these results as given by

$$\rho_s = \rho_M \frac{\Re_s - \Re_0}{\Re_M - \Re_0} \tag{1}$$

where ρ_s is the sample (Pyro #1 or #3) reflectance, ρ_M is the standard mirror reflectance, $\Re_s$ is the ratio of sample to reference measurements, $\Re_M$ is the ratio of standard mirror to reference measurements, and $\Re_0$ is the ratio of empty aperture to reference measurements.

The measurements of the bare detector and KRS5 window were made without the motorized stages, were aligned "by eye", and employ our standard reference measurement. For the final results on these elements, we also used fixed apertures as described above, but did not require the gold mirror measurement.

3.3.2 Calculation of the detector effective absorptance

3.3.2.1 Pyroelectric detector reflectance.

Pyro #1 and #3 reflected flux consists primarily of two components: 1) flux reflected by the KRS5 window, and 2) flux transmitted through the KRS5 window, reflected by the detector element and transmitted back through the window. There are also higher order inter-reflections between the window and detector, but their contributions are insignificant (<0.001) for the black-coated detector. Then the measured Pryo #1 or #3 reflectance is given by

$$\rho_{PyroCalc} \approx \rho_{KRS5} + \tau_{KRS5}^2 \rho_{\text{det}} \tag{2}$$

where ρ_{KRS5} and τ_{KRS5} are the reflectance and transmittance of the KRS5 window, respectively. $\rho_{PyroCalc}$ is the calculated windowed detector reflectance, and ρ_{det} is the bare detector reflectance.

In Fig. 6, a comparison of the measured reflectance of the two pyroelectric detectors from Equation (1) and that calculated from Equation (2) is shown. Pyro #1 and Pyro #3 are denoted as "Det 1" and Det 3". Note that the measured reflectances of the two detectors match at long wavelengths and gradually diverge at shorter wavelengths. This is characteristic of greater scattering in the window of Pyro #1. The calculated reflectance, based on the bare detector and KRS5 window measurements, matches the detector 3 result at shorter wavelengths, indicating that the KRS5 window of Pyro #1 is similar to the test window. Note also that the structure in the measured reflectance of the two detectors is significantly less than seen in the calculated spectrum. This inconsistency can be resolved by the following considerations.

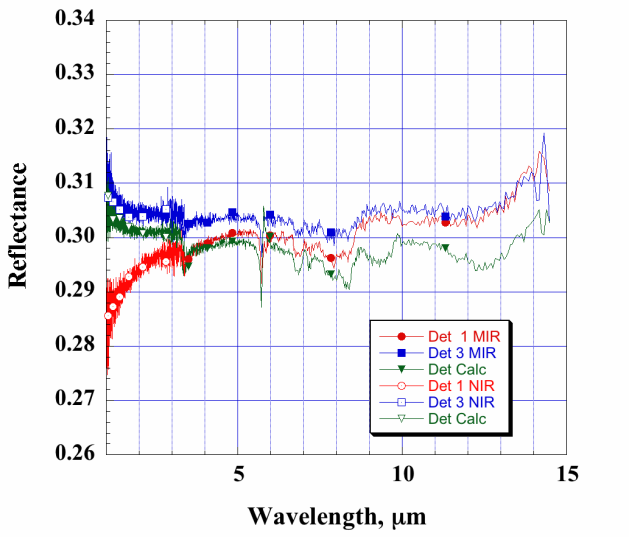

Fig. 6 Comparison of directly measured and calculated reflectance of detector packages.

First, not all of the flux reflected by the detector element and penetrating the window gets through the window to be measured as reflected by the sphere. This is because the detector coating reflects flux diffusely, so that some of the flux is absorbed and reflected by the detector can. So we need to include a factor to account for the loss:

$$\rho_{Pyro\#} \approx \rho_{KRS5} + \tau_{KRS5}^2 \rho_{\text{det}} f_{loss} \tag{3}$$

If we let f_{loss} vary and adjust it to so that the depth of the simple absorption structure near 6 μmin the calculated spectrum, which is associated with the bare detector, matches that in the measured spectra, we find $f_{\text{loss}} \approx 0.5$.

Secondly, the KRS5 window exhibits some scattering of flux, in which case flux can be trapped in the window and channeled to the edges, where it is not detected in either a transmittance or reflectance measurement. This was seen in the KRS5 window characterization, in which the sum of the window transmittance and reflectance is found to be about 0.99 across most of the spectrum, except at short wavelengths, where it decreases further. In addition, some light, which is transmitted will miss the bare detector due to scattering. We handle this effect by letting

$$\rho_{KRS5-i} = \rho_{KRS5} + \Delta\rho_{KRS5-i} \tag{4}$$

and

$$\tau_{KRS5-i} = \tau_{KRS5} - \Delta\rho_{KRS5-i} \tag{5}$$

where ρ_{KRS5} and τ_{KRS5} are the measured window reflectance and transmittance, respectively, $\rho_{KRS5\text{-}i}$ and $\tau_{KRS5\text{-}i}$ are the reflectance and transmittance of the window for Pyro #*i*, the subscript *i* denotes detector 1 or 3, and $\Delta\rho_{KRS5\text{-}i}$ is the reflectance difference between the windows. Using our measured results and Equations (3) – (5), we calculate $\Delta\rho_{KRS5\text{-}i}$,

$$\Delta\rho_{KRS5-i} \approx \frac{(\rho_{Pyro\#i} - \rho_{KRS5}) + \tau_{KRS5}^2 \rho_{\det} f_{loss}}{(1 - 2\tau_{KRS5}\rho_{\det} f_{loss})} \quad (6).$$

3.3.2.2 Detector effective absorptance.

As in the case of the Pryo #*i* reflectance, two terms are sufficient to account for > 0.999 of the light absorbed. These terms are from the initially incident light on the bare detector element and the subsequent first inter-reflection between the detector and window. The effective absorptance, α'_i, is then given by:

$$\alpha'_i = (1 - \rho_{\det})\tau_{KRS5-i}(\rho_{KRS5-i}\rho_{\det} f_{loss} + 1) \quad (7)$$

If we combine Equations (4) – (7), and assume that the detector responsivity is proportional to its effective absorptance, we then obtain the relative detector responsivity in terms of measured quantities:

$$\Re_i / C_i = (1 - \rho_{\det})\tau_{KRS5}(\rho_{KRS5}\rho_{\det} f_{loss} + 1) + \frac{(1 - \rho_{\det})((\tau_{KRS5} - \rho_{KRS5})\rho_{\det} f_{loss} - 1)(\rho_{Pyro\#i} - \rho_{KRS5} + \tau_{KRS5}^2 \rho_{\det} f_{loss})}{(1 - 2\tau_{KRS5}\rho_{\det} f_{loss})} \quad (8)$$

where $\Re_i$ is the i_{th} detector responsivity and C_i is a proportionality constant which depends on other characteristics of the i_{th} detector such as detector thickness, etc., but which is independent of wavelength and hence constant. The results of calculations from Equation 8 are shown in Fig. 7.

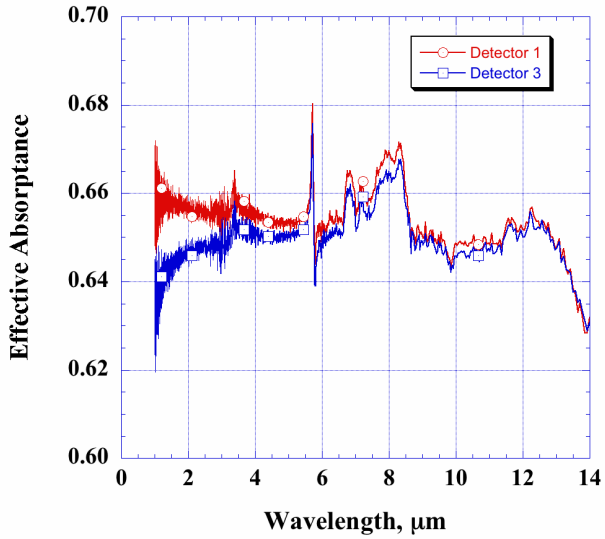

Fig 7. Effective absorptance of Pyro #1 and #3. This is directly proportional to the relative spectral responsivity.

3.4 DETECTOR SPECTRAL RESPONSIVITY RESULTS

3.4.1 Combining SIRCUS and FTIS Results

We obtain the absolute spectral responsivity by combining the relative spectral responsivity from Figure 5 and absolute spectral responsivity at specific wavelengths from Figure 2. An overlay of the two data sets is shown in Fig. 8 (a) and (b), where (a) shows the near infrared spectral region detail. Note that the responsivities of the two detectors are nearly identical at the shortest wavelength (785 nm) measured. Due to the limitations of the infrared spectral reflectance instrument, the spectral data below 1 micron becomes increasingly noisy. However, to the extent that no spectral structure is expected, the data can be smoothed; also, it would be reasonable to extrapolate the data below 833 nm down to the 785 nm laser tie point.

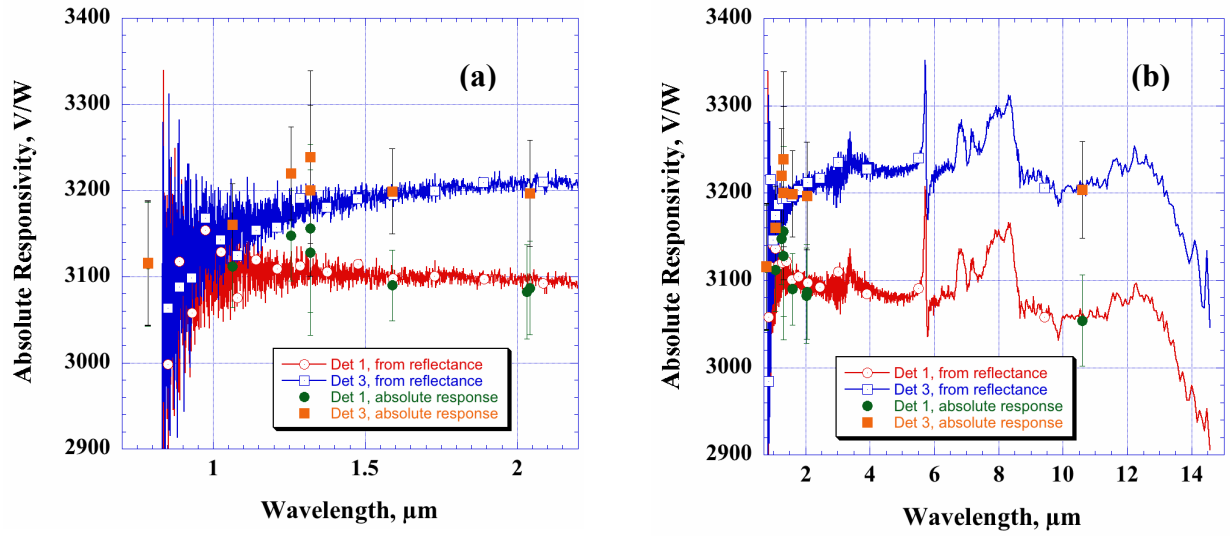

Fig. 8 Absolute spectral responsivity of pyroelectric test detectors Pyro #1 and Pyro #3; (a) near IR detail, and (b) full spectral range.

Normally we calculate the uncertainties for the *absolute* spectral reflectance or absorptance. However, for the detector spectral responsivity determination, we only need to know the *relative* spectral variation in the absorptance and hence only the uncertainty components associated with the relative variation need to be included in the uncertainty budget. The primary uncertainty terms for this relative absorptance are the noise and unaccounted for effects of scattering in the window and inter-reflections within the detector package.

3.5 Calibration uncertainty analysis summary

3.5.1 Result of error analysis of direct calibration

The uncertainty components of the direct calibration come from spatial non-uniformity, laser stability, AC-DC conversion, ambient temperature variation, wavelength variation of the tunable laser, repeatability etc. The uncertainty associated with the direct calibration is approx. 2 % ($k = 2$).

3.5.2 Result of error analysis of relative spectral measurement

The main contributions to the uncertainty of the relative spectral responsivity from the FTIS characterization is the variation of the KRS5 window transmittances, the variation of the reflectance of the detector elements and the unknown inter-reflection processes within the windowed detectors. The incorporation of multiple tie-points of several wavelengths validate the relative curves and reduce the uncertainty approx. 1 % ($k = 2$).

4. CONCLUSIONS

We have calibrated the spectral responsivity of two commercially available KRS5 windowed pyroelectric detectors through the use of NIST ACR L1, the domed pyroelectric transfer standard radiometer, and FTIR spectral measurement facilities. The pyroelectric detectors have been spatially mapped to accommodate the spatial non-uniformity caused by interference fringes at 10.6 μm. The absolute responsivity of the windowed detectors at several wavelengths across the spectrum is obtained by directly comparing against the ACR L1 and transfer standard radiometer in the wavelength range from 785 nm to 2000 nm and at 10600 nm. The effective absorptance spectra of the detector packages were measured by FTIR, incorporating measurements of the reflectance of the bare detector surface and the reflectance and transmittance of a KRS5 window, as well as the reflectance of the windowed detectors under test. The final spectral responsivity of the two windowed pyroelectric detectors is determined by combining the effective absorptance and the absolute responsivity at several wavelengths. The multiple tie points are used to assess and validate the calculated effective relative response spectra. The relative spectral responsivity from FTIR measurement is consistent with the results of ACR and transfer standard calibrations. The uncertainty is determined to be less than 2 %.

REFERENCES

[1] G. Eppeldauer, J. Zeng, and L.M. Hanssen, "Development and calibration of pyroelectric radiometer standards at NIST," Proc. SPIE **6201**, 620119 (2006).

[2] G. P. Eppeldauer, J. Zeng and L. M. Hanssen "Spectral responsivity scale between 1 μm and 19 μm at NIST," in Proc. NEWRAD 2005, ed. by J. Groebner, PMODWRC, Davos, Switzerland, 241-242 (2005).

[3] Lykke K. R., Shaw P.-S., Hanssen L. M., and Eppeldauer G. P., " Development of a monochromatic, uniform source facility for calibration of radiance and irradiance detectors from 0.2 μm to 12 μm," Metrologia, **35**, 479-484 (1998).

[4] H. Gong, L. M. Hanssen and G. P. Eppeldauer, "Spatial and angular responsivity measurements of photoconductive HgCdTe LWIR Radiometers," Metrologia, **4**, 161-166 (2004).

[5] L.M. Hanssen, "Integrating-sphere system and method for absolute measurement of transmittance, reflectance, and absorptance of specular samples," Applied Optics **40** (19), 3196-3204 (2001).

[6] L.M. Hanssen, and S.G. Kaplan, "Linearity characterization of NIST's infrared regular transmittance and reflectance scales," Proc. SPIE **4826**, 21-26 (2003).